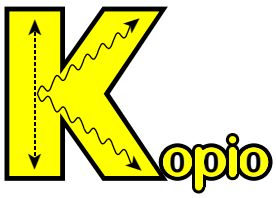

KOPIO note tn027, October 2001

Measurements on the response of plastic scintillator to charged pions at 185 - 360 MeV/c

Charged-particle veto R&D

Heinz Kaspar, Peter Robmann, Andries van der Schaaf, Simon Scheu, Peter Truöl
Physik-Institut der Universität Zürich, CH-8001 Zürich

Johny Egger
Paul Scherrer Institut, CH-5232 Villigen

Marvin Blecher
Virginia Polytechnic Institute and State University, Blacksburg, VA 24061, USA

1 Introduction

1.1 the Kopio [1] charged-particle veto system

The purpose of the charge-particle veto system is the efficient identification of background processes in which an apparent $\pi^0 \to 2\gamma$ decay inside the decay volume is accompanied by charged particle emission. Examples of such background processes are, (i) $K_L \to \pi^+\pi^-\pi^0$, (ii) $K_L \to e^+\pi^-\nu\gamma$ in which the positron creates a second photon through Bremsstrahlung or annihilation in flight, (iii) $K_L \to e^+\pi^-\nu$ again followed by $e^+ \to \gamma$ whereas the π^- creates a photon through $\pi^- p \to \pi^0 n$. In all cases two particles with opposite electrical charge emerge. In all cases the events may also produce signals in other detector elements, like the barrel veto system. Detection efficiencies of 99.99% or better are required to keep these backgrounds below a few events in the final sample.

The charged-particle veto system will consist of two or three layers of plastic scintillator mounted inside the vacuum tank surrounding the decay volume. The detectors will be separated from the high-quality beam vacuum by a thin metallic foil.

1.2 tests with beam

In spring 2001 we measured the response of plastic scintillator to $\pi^\pm$, $\mu^\pm$ and $e^\pm$ at momenta between 185 and 360 MeV/c. These studies are a first step towards a better understanding of the fundamental limitations to the detection efficiency of the charged-particle veto system. Such limitations are associated with processes (like pion absorption, pion back scattering, or positron annihilation in flight) that result in a partial or complete loss of scintillator signal. We also tested detector prototypes, in particular of scintillators with embedded wave-length-shifting fibres. In this note we present results on pion inefficiencies. Muon and electron inefficiencies were found to be much lower and in most cases only upper limits could be determined. For this reason we intend to take more data before presenting any results for these particles. Experience gained with the detector prototypes will be communicated in another KOPIO note.

2 Setup and data taking

Figure 1 shows the experimental setup which consists of a particle defining telescope (counters 1-3 and

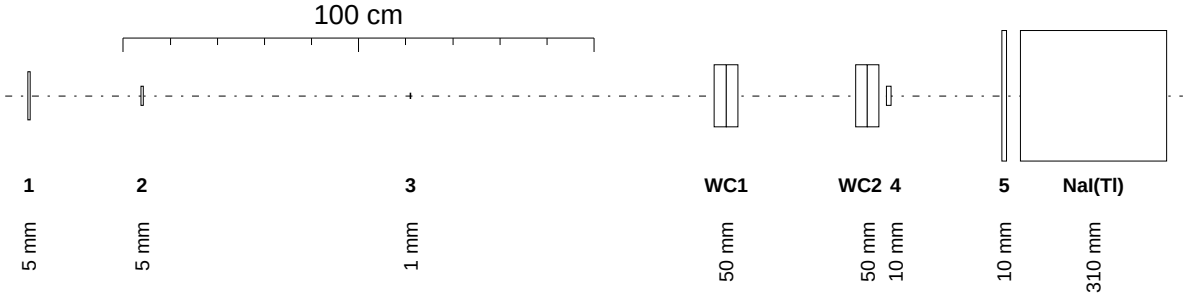

Figure 1: *Experimental setup for the measurements of the response of plastic scintillator to $\pi^{\pm}$, $\mu^{\pm}$ and $e^{\pm}$. 1-5: plastic scintillation detectors; WC1/2: x-y proportional wire chambers with 1mm wire spacing. The values on the bottom denote the thickness of the corresponding detector. The beam extracted from the πM1 channel at PSI enters from the left.*

$x-y$ multi-wire proportional chambers WC1 and WC2) followed by a veto system consisting of two plastic scintillation detectors (4 and 5) and a NaI(Tl) crystal.

Data were taken at beam momenta between 185 and 360 MeV/c for both polarities. The beam intensity was kept below $\approx 5 \times 10^3$ s^{-1} with the help of slits along the πM1 beam line and by detuning the first quadrupoles of the channel. The trigger for data readout required signals in counters 1 and 3. Amplitude and time information for all scintillation detectors, the wire hits in WC1/2 and the phase with respect to the 50 MHz cyclotron r.f. signal were recorded. The latter information was used offline to discriminate between pions, muons and electrons in the beam.

3 Track analysis

Offline events were selected with WC1/2 trajectories pointing at counter 3. (see Fig. 2). In case of ambiguous wire chamber information it was required that at least one solution satisfied the selection

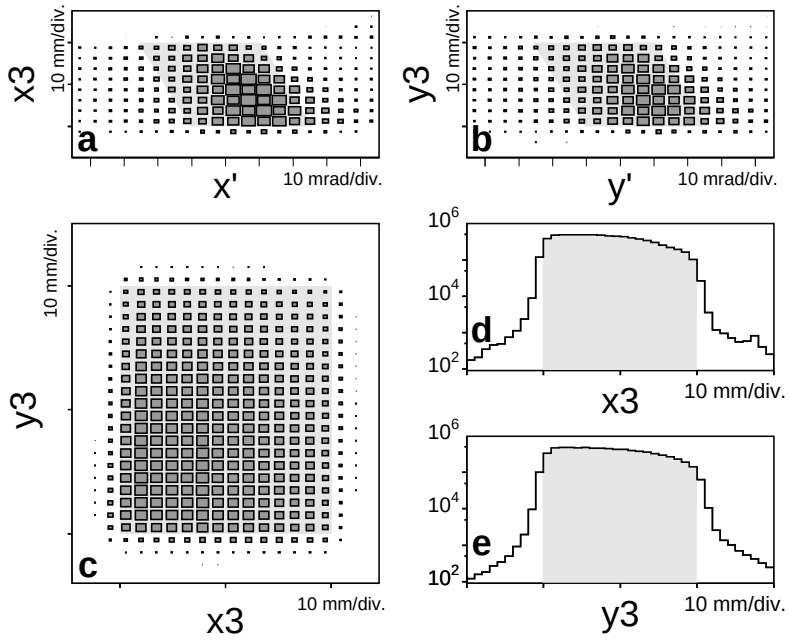

Figure 2: *Distributions of the divergences $x\prime$ and $y\prime$ and the trajectory coordinates extrapolated to counter 3. Only events from the shaded areas were accepted for further analysis.*

criteria. At a later stage (see Sec. 7) we study the nature of the events with extra WC2 hits.

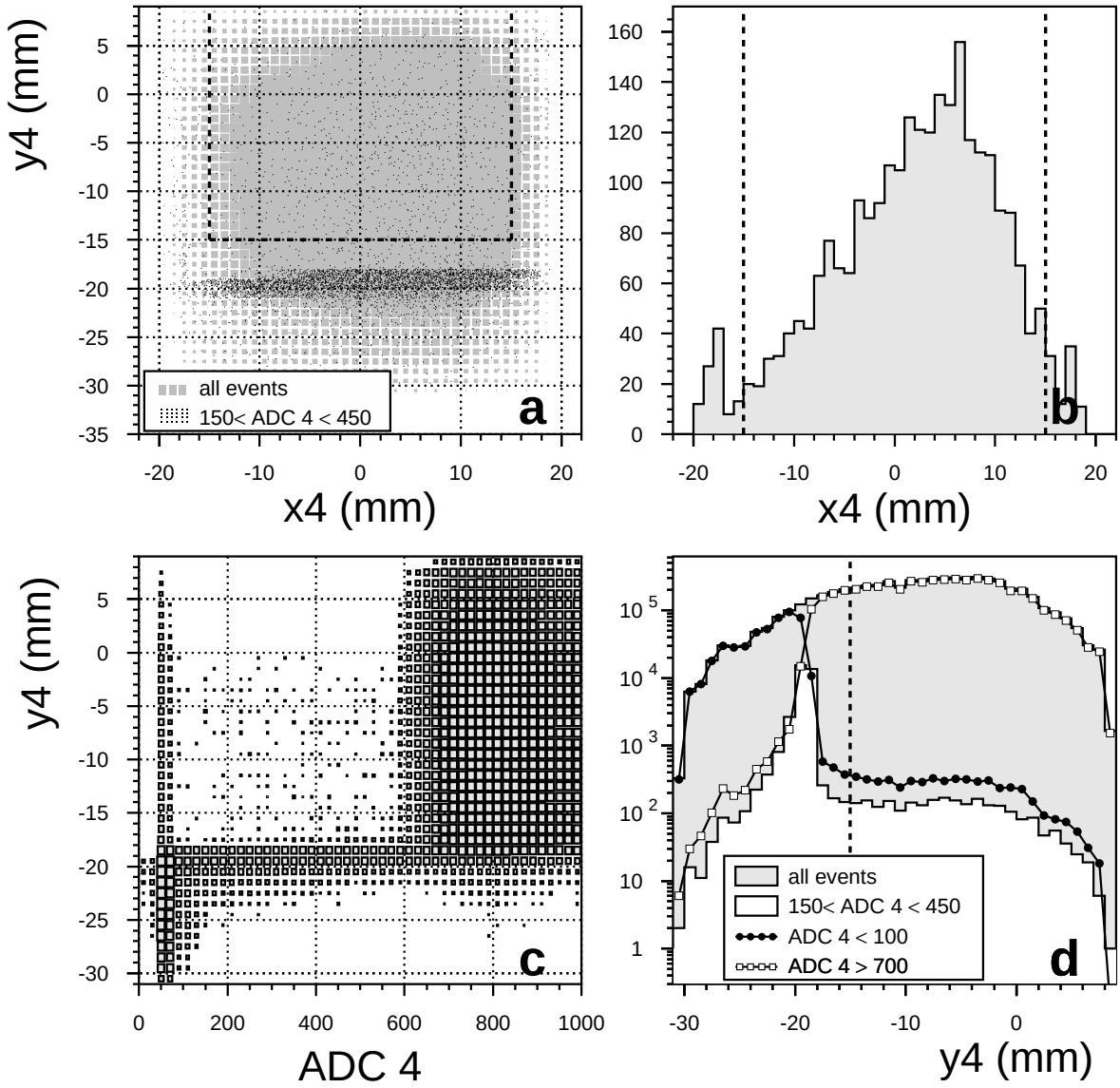

Figure 3: *Distributions of (x4,y4), the coordinates of the trajectory on counter 4, and ADC 4, the observed charge from the photo-multiplier. Events at all momenta and all particle types have been included. In part a the grey distribution shows the spot resulting from the selection by counter 3. The black distribution is for events with small signals which enhances the scintillator edges. Part b show a slice of this distribution with y4≥-15 mm. Part c shows the change in response around y4=-20 mm where the scintillator is glued to the light guide. Part d shows slices of c. Dashed lines indicate the selection cuts $|x4|, |y4| \leq 15$ mm, selecting the central 30×30 mm^2 of counter 4.*

Figure 3 shows the response of counter 4 as a function of the position $(x4, y4)$ on the detector. One notices that the selected spot is centred around $y4 \approx -7$ mm resulting from a misalignment of counters 3 and 4. As a result in some 10% of the events the particle crossed the light guide of counter 4 situated in the region $y4 \leq -20$ mm. Events with $(x4, y4)$ coordinates inside the central 30×30 mm^2 were selected for further analysis. As before in case of ambiguities at least one $(x4, y4)$ solution had to fulfil the requirements.

4 Particle identification

Particle identification was done on the basis of time of flight (TOF) between the production target and detector 2, i.e. a distance of 24.5 m. Given the 50 MHz rf structure of the PSI cyclotron the observable is Δt_{rf} ≡mod(TOF,20 ns). Figure 4 shows the observed distributions. At the highest momentum

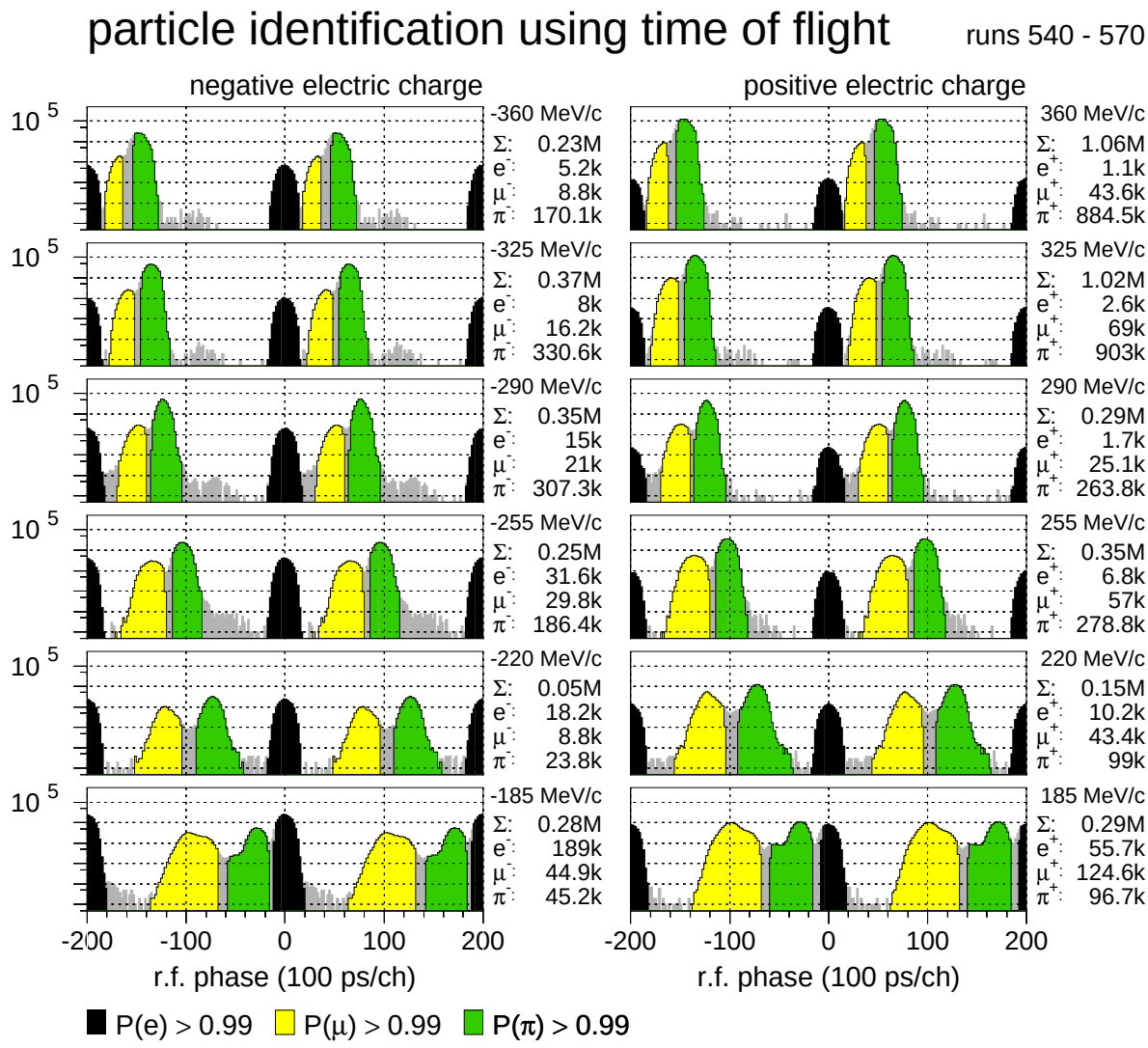

Figure 4: *Distributions of Δt_{rf} (see text) for the various beam momenta. For convenience two periods are shown so each event enters twice. Indicated are the regions where particle identification is possible with 99% confidence or better. The resulting sample sizes are indicated in the margin.*

(360 MeV/c) pions and muons can still be resolved. At the lowest momentum (185 MeV/c) pions arrive just before electrons from the next beam bucket.

5 Response to pions

Figure 5 shows the NaI(Tl) energy distributions for $e^{\pm}$ and $\pi^{\pm}$. The muon spectra are very similar to those observed for $e^{\pm}$. Whereas >99% of the electrons and positrons produce signals in the full-energy

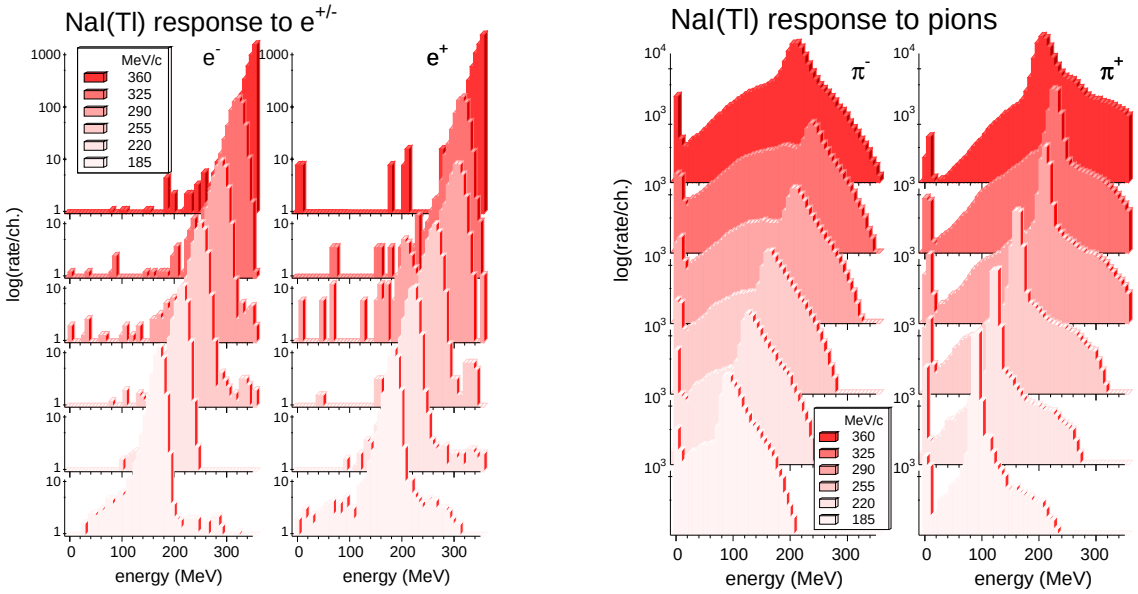

Figure 5: *NaI(Tl) response to $e^{\pm}$ and $\pi^{\pm}$ at various momenta in the range 185-360 MeV/c. Particles were selected with signals in counters 1-3 and WC1/2 with trajectories pointing at counter 4. All spectra have been normalised to 100000 entries. At 360 MeV/c pions may cross the detector resulting in a reduction in energy deposit.*

peak with no indication of a pedestal peak, pions may disappear by nuclear reactions resulting in a broad continuum with an endpoint corresponding to the total pion energy. In 1-3% of the cases no signal is seen at all. These events are caused by interactions in counters 4 and 5 (total thickness 20 mm)

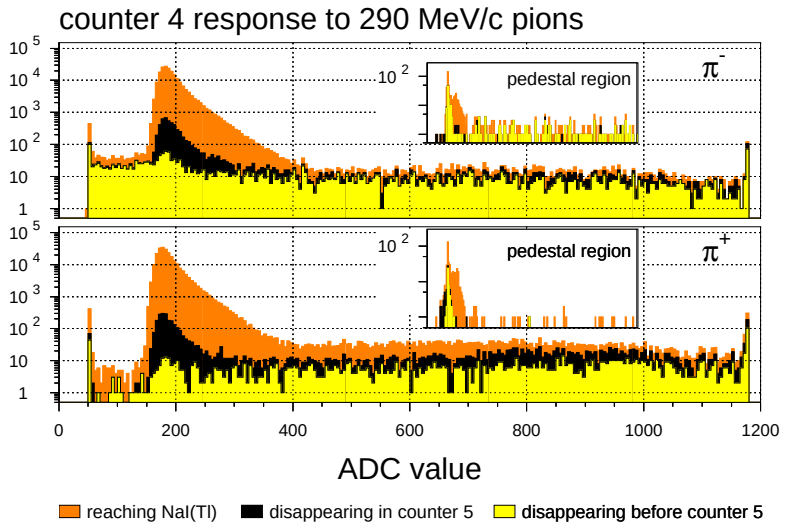

Figure 6: *Response of counter 4 to 290 MeV/c $\pi^{\pm}$ for, (i) all events with trajectories pointing at counter 4, (ii) the subset of (i) contained in the NaI(Tl) pedestal peak (see Fig. 5), and (iii) the subset of (ii) contained in the pedestal peak of counter 5. The inserts give expanded views of the pedestal region 50<ADC<100.*

Figure 6 shows various distributions of the signals produced by 290 MeV/c pions in counter 4. Similar spectra are observed at the other momenta. Events without signals in counter 5 and NaI(Tl) are characterised by flat distributions with a small peak contribution caused by interactions in the dead layer between counters 4 and 5. Note the striking difference between π^+ and π^- in the event rate at the low side of the peak: whereas π^- interactions often lead to neutral final states π^+ is known to produce one or more low-energy protons [2] which result in additional scintillation light.

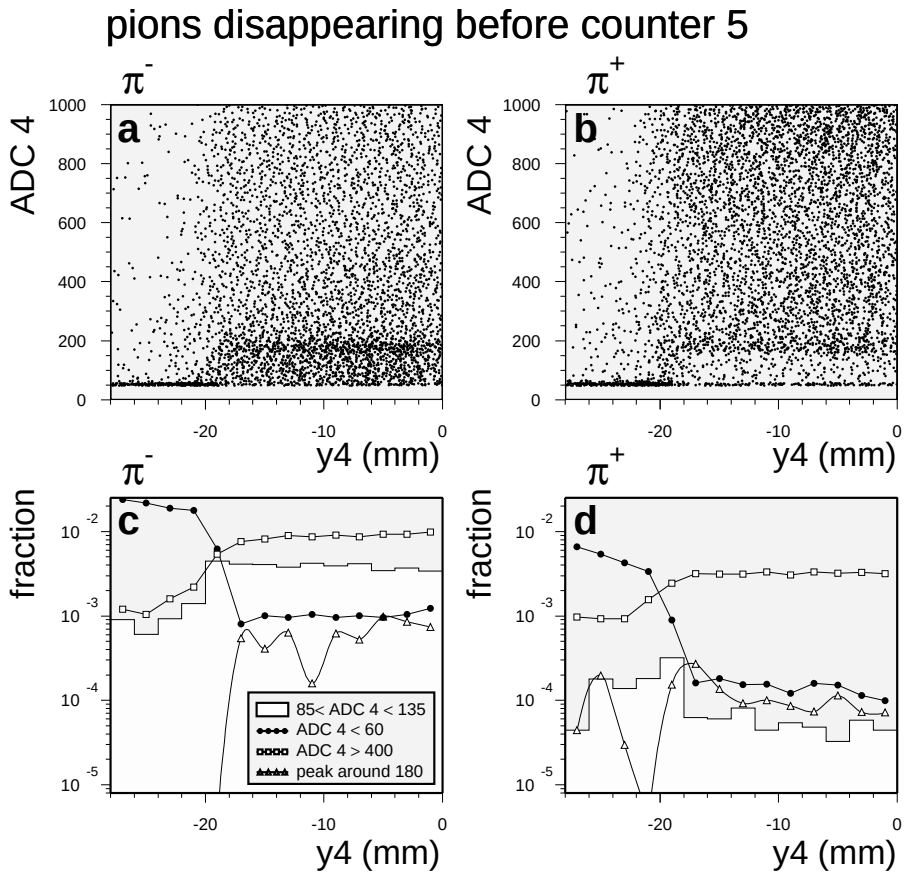

Figure 7: *Distributions of the signal in counter 4 versus y4 for π^- and π^+ giving no signals in counter 5 and NaI(Tl). Data from the different momenta have been included. Notice the distinct structure at y4=-20 mm where the light guide connects to the scintillator. "Fraction" in parts c and d is the distribution of the events in a given ADC window normalised to the incoming pion flux (without veto by counter 5 and NaI(Tl)).*

More detailed information is found in Fig.7 which shows the dependence of the signal in counter 4 on $y4$ (see Sec. 2) for pion induced events without signals in counter 5 and NaI(Tl). $y4$-Distributions of four subsets of the data are shown for π^+ and π^- separately (see Fig. 8 for illustrations):

- Pedestal events (ADC<60), i.e. events without any signal in counter 4. These events are caused by interactions in WC2, the wrapping of counter 4 and the light guide. The latter events have a very prominent contribution of $O(\%)$ below $y4$=-20. For trajectories pointing at the scintillator ($y4$ >-20) fractions in the region $10^{-3} - 10^{-4}$ are observed. See Sec. 7 for further discussion.
- Large-signal events (ADC>400), i.e. events in which protons or other nuclear fragments reached the detector. Since part of these events are caused by pion interactions upstream of counter 4 the slope at $y4$ =-20 is broadened.

- Small-signal events (85<ADC<135). Whereas π^- induced events show a clean scintillator image resulting from (π^-,2n) and (π^-, π^0) reactions the π^+ data are rather structureless. For this reason we analyse the "peak" events as an independent measure of the dead-layer effect.

- Peak events (enhancement at ADC$\approx$ 185), i.e. events in which pions traverse counter 4 (thus situated in the corresponding peak, see Fig.6) and disappear before reaching scintillator 5. These events, having fractions similar to the pedestal events, do show an image of counter 4 without the strong enhancement due to the light guide.

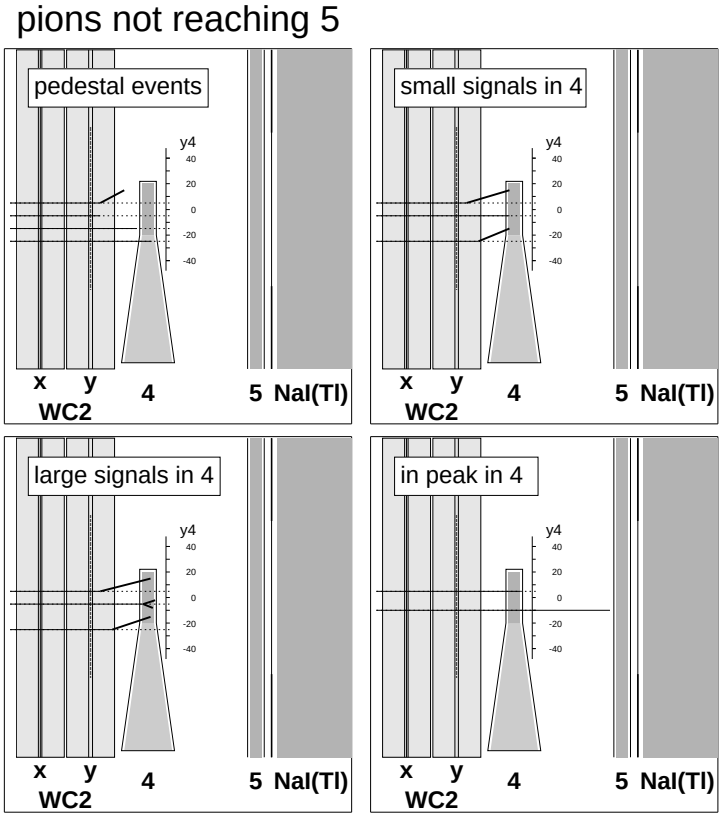

Figure 8: *Examples of various processes in which pions disappear before reaching counter 5.*

6 Simulation

The GEANT simulation geometry (see Fig. 1) included WC2, counters 4 and 5, NaI(Tl) and all the wrappings. Pions were started at the upstream side of WC2 in a parallel beam. The tracking was done with the GCALOR package for hadronic interactions. All electromagnetic interactions and decays were allowed.

The simulation logic assumed that WC2 provided two values of (x,y,z), determined from the average of the entrance and exit positions of a charged particle passing through the planes. Only events with one entering and one exiting track in each plane were considered. If the track did not point to the active area of counter 4 (see Fig. 3) the event was eliminated.

For the selected events the energy deposited in counters 4 and 5, and NaI(Tl) was histogrammed and good agreement with the measured distributions was observed. In particular the observed ratio of 1:2 between the contributions to the peak and the continuum in the NaI(Tl) spectrum (see Fig. 5) could be described. In addition the counter 4 distributions of Fig. 6 were reproduced and analysed as done for the measured data. The resulting inefficiencies are presented and discussed in Sec. 7.

7 Results and discussion

The observed pion detection inefficiencies are plotted against beam momentum in Fig. 9. Four different cases have been analysed: with/without veto by NaI(Tl) and WC2. Veto by WC2 means that events are rejected with more than one hit in the last WC2 plane. When vetoing with NaI(Tl) one recognises

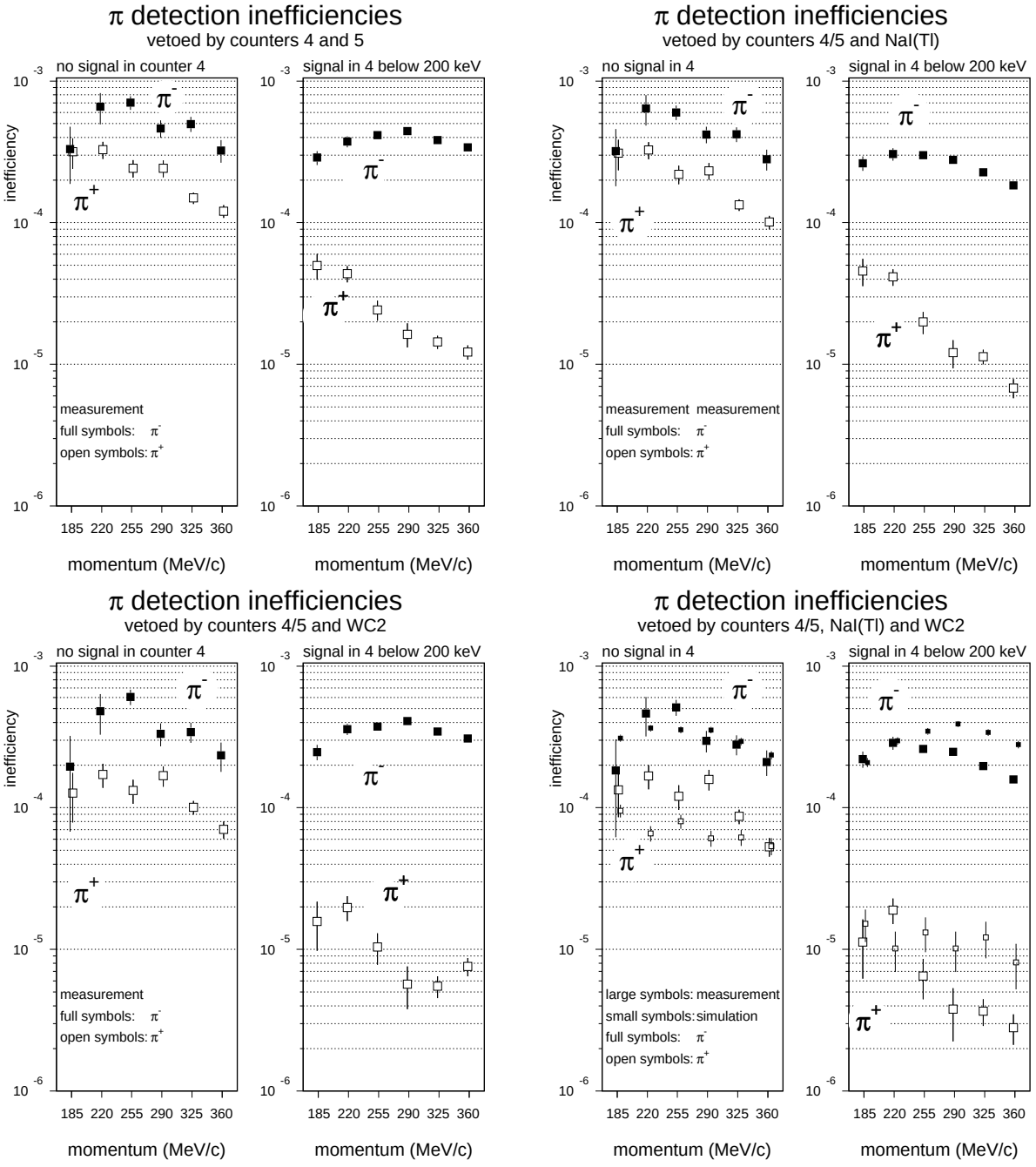

Figure 9: *Pion detection inefficiency caused by interactions in WC2 and the wrapping of counter 4 and by a 200 keV detection threshold on the signal in counter 4. On the left side results are shown for the case that counter 5 is used as veto counter too. On the right side also NaI(Tl) is used as veto counter. In all distributions a good track was required. For the bottom distributions events with more than one hit in the downstream wire chamber plane were rejected.*

part of the single charge exchange leading to $\pi^0 \rightarrow 2\gamma$. When vetoing on additional WC2 hits one removes part of the interactions in WC2 but also events with back-scattered pions or secondaries.

In all four cases the inefficiency is split into two contributions: no signal in counter 4 (ADC value in pedestal peak) or signal below 200 keV (one tenth of the mean energy deposited by a through-going pion). Results from the simulation of case 4 are indicated. Compared to the most conservative procedure which considers counters 4 and 5 only, the information from WC2 and NaI(Tl) improves the results by a factor 2 at best, except for π^+ events with small counter 4 signals where the apparent inefficiencies drop by a factor $\approx$5. We have checked the distributions of a second hit in WC2 and found only for π^+ a significant component of correlated hits located wothin a few cm from the main track. Otherwise the additional hits are mostly uncorrelated.

In the case of π^- the losses caused by the dead layer and 200 keV threshold are similar which can be understood if one assumes that the dominant contribution comes from π^- absorption into neutrals. In the case of π^+ pion absorption mostly leads to final states with one or more protons [2]. Since those tend to be emitted isotropically at relatively low momenta dead-layer absorption has a non-negligible probability to produce no signal in counter 4. When absorption takes place inside the scintillator the process generally leads to an increased signal which explains the very low inefficiency associated with the 200 keV detection threshold.

The simulation reproduces the observed inefficiencies within a factor two which we consider satisfactory in view of the complexity of the problem. Simulation shows that about 2/3 of the dead-layer losses are caused by the wrapping of counter 4 which amounts to 55 mg/cm^2. This means that the values plotted in Fig. 9 correspond to a dead layer of $\approx$ 80 mg/cm^2.

7.1 Nature of inefficiencies observed in simulation

We checked twenty simulated events in which no energy was deposited in counter 4 or where this energy was below 75 keV. These events had no energy in NaI(Tl) and only one hit per plane in WC2.

- π^+ **inefficiency**. Out of ten events:
  - there were six cases in which the pion was scattered into the backward hemisphere without reaching WC2. The pions were left with sufficient energy to fire a scintillator and would have been detected by a system covering the full solid angle. In one of these events the pion made a reaction in the scintillator. In the remaining five events there were hadronic interactions in the wrapping with final states containing up to 3 gammas, up to 2 neutrons, up to 2 protons and sometimes even 1-2 alpha particles. The charged particles typically stopped in the wrapping.
  - there were four cases with a π^0 in the final state without signal in counter 4. In the experiment the decay gammas would be detected in the barrel vetos or calorimeter.

  We conclude that a large fraction of the π^+ losses observed in the test are associated with scattered pions. Pion scattering has a differential cross section of $\approx$20 mb/sr almost independent of scattering angle [3]. Most of these events would not contribute to the inefficiency of a hermetic veto system. The π^+ inefficiencies would be dominated by the effect of the dead layer. Since that layer would be 2-3 times thinner in the real setup values significantly below 10^{-4} could be obtained.

- π^- **inefficiency**. Out of ten events:
  - in seven cases the pion disappeared in the wrapping and there were neutrons and maybe a π^0 in the final state. There are also unseen gammas, a possible proton, and an alpha particle. The charged particles stopped in the wrapping as for π^+.
  - in three cases the pion reached the scintillator. In one of them the pion was scattered backward.

Losses are mainly caused by (π^-,xn) absorption so in this case our results should be considered realistic.

8 Detector requirements

Detection inefficiencies for π^- below 2×10^{-4} at the most critical momenta around 250 MeV/c would require:

- a dead layer in front of the veto system (which includes the window separating the detector from the high-vacuum decay region) below 20 mg/cm^2 and
- a detection threshold of $\approx$ 75 keV.

Meeting this performance seems neither trivial nor hopeless. The most critical parameter is the yield of photo electrons per energy deposit. First tests indicate a value of $\approx$ 100 photo-electrons for minimum ionising particles crossing 10 mm of scintillator read out with embedded w.l.s. fibre. This corresponds to three photo electrons for a 75 keV threshold. The sensitivity of counter 4 which was viewed through a classical fishtail light guide is about 20 times higher and for this reason we intend to make a critical comparison between full-scale prototypes of both types of detector.

References

[1] *Rare Symmetry Violating Processes*
Joined MECO/KOPIO proposal (1999), `http://pubweb.bnl.gov/people/rsvp`.

[2] *Positive-Pion Absorption by C Nuclei at 130 MeV*
E. Bellotti *et al.*, Il Nuovo Cimento **18A**, 75 (1973).
Pion absorption reactions on N, Ar and Xe
B. Kotlinski *et al.*, Eur.Phys.J. A **9**, 537 (2000).

[3] *Quasielastic scattering of pions from ^{16}O at energies around the $\Delta(1232)$ resonance*
C.H.Q. Ingram *et al.*, Phys. Rev. **C27** (1983) 1578.